

New approach to the thermal Casimir force between real metals

V. M. Mostepanenko^{1,2} and B. Geyer¹

¹Center of Theoretical Studies and Institute for Theoretical Physics, Leipzig University, D-04009, Leipzig, Germany

²Noncommercial Partnership “Scientific Instruments”, Tverskaya St. 11, Moscow, 103905, Russia

Abstract. The new approach to the theoretical description of the thermal Casimir force between real metals is presented. It uses the plasma-like dielectric permittivity that takes into account the interband transitions of core electrons. This permittivity precisely satisfies the Kramers-Kronig relations. The respective Casimir entropy is positive and vanishes at zero temperature in accordance with the Nernst heat theorem. The physical reasons why the Drude dielectric function, when substituted in the Lifshitz formula, is inconsistent with electrodynamics are elucidated. The proposed approach is the single one consistent with all measurements of the Casimir force performed up to date. The application of this approach to metal-type semiconductors is considered.

PACS numbers: 05.30.-d, 77.22.Ch, 12.20.Ds

1. Introduction

The Casimir force [1] acts between two parallel electrically neutral metal plates in vacuum. This effect is entirely quantum. There is no such force in classical electrodynamics. In accordance to quantum field theory, there are zero-point oscillations of the electromagnetic field in the vacuum state. The Casimir effect arises due to the boundary conditions imposed on the electromagnetic field on metal surfaces. The spectra of zero-point oscillations in the presence and in the absence of plates are different. Casimir was the first who found the finite difference between respective infinite vacuum energies. The negative derivative of this difference with respect to the separation between the plates is just what is referred to as the *Casimir force*.

In his famous paper [1] Casimir considered ideal metal plates at zero temperature. Modern progress in measurements of the Casimir force (see early stages in review [2] and later experiments [3, 4, 5, 6, 7, 8, 9]) demand consideration of realistic plates of finite conductivity at nonzero temperature. This is also of much importance for the applications of the Casimir effect in nanotechnology [10, 11]. The basic theory of both the van der Waals and Casimir force taking into account the effects of finite conductivity and nonzero temperature was developed by Lifshitz [12]. It describes material properties

by means of the frequency dependent dielectric permittivity. First applications of this theory at nonzero temperature using the Drude [13] and plasma [14, 15] models for the dielectric permittivity have led, however, to contradictory results. In particular, thermal Casimir force if calculated using the Drude model was found to be in qualitative disagreement with the case of ideal metals. The large thermal correction arising at short separation distances within this approach was excluded experimentally [5, 6, 7]. In addition, the Casimir entropy calculated using the Drude model violates the third law of thermodynamics (the Nernst heat theorem) for perfect crystal lattices with no impurities [16, 17]. As to the nondissipative plasma model, it leads to the thermal Casimir force in qualitative agreement with the case of ideal metals and satisfies the Nernst theorem. It was found to be consistent with the data of relatively large separation experiments on the measurement of the Casimir force [5, 6, 7]. However, as is demonstrated below in Section 2, it is in contradiction with the results of short separation experiment [18]. This can be explained by the fact that the plasma model completely disregards interband transitions of core electrons. Another approach to the thermal Casimir force is based on the use of the Leontovich surface impedance instead of dielectric permittivity [19]. This approach is consistent with thermodynamics and large separation experiments, but it is not applicable at short separations.

In this paper we present and further elaborate a new theoretical approach to the thermal Casimir force based on the use of generalized plasma-like dielectric permittivity [20]. We demonstrate that this approach is consistent with all available experimental results. Physical reasons why the Drude dielectric function is not compatible with the Lifshitz theory in the case of finite plates [21] are discussed. We demonstrate that results obtained in [21] have far reaching consequences not only for metals but also for semiconductors of metallic type with sufficiently high dopant concentration.

In Section 2, on the basis of fundamentals of statistical physics and all available experimental data we explain why the new approach to the thermal Casimir force is much needed. Section 3 explains the effect of finite plates, i.e., that the Drude dielectric function is not applicable when the front of an incident wave has much larger extension than the size of the plate. Section 4 contains the formulation of the generalized plasma-like dielectric permittivity. The results of a recent 6-oscillator fit to its parameters (see Ref. [7]) using the tabulated optical data for Au [22] are also presented. In Section 5 we compare the generalized Kramers-Kronig relations valid for the plasma-like permittivity with the standard ones valid for dielectrics and for Drude metals. Section 6 briefly presents the thermodynamic test for the generalized plasma-like permittivity. In Section 7 we apply the developed approach to the case of semiconductors with relatively high concentration of charge carriers. Section 8 contains our conclusions and discussion.

2. Why a new approach is needed?

We start with the Lifshitz formula for the free energy of the van der Waals and Casimir interaction between the two parallel metallic plates of thickness d at a separation

distance a at temperature T in thermal equilibrium

$$\mathcal{F}(a, T) = \frac{k_B T}{2\pi} \sum_{l=0}^{\infty} \left(1 - \frac{1}{2}\delta_{0l}\right) \int_0^{\infty} k_{\perp} dk_{\perp} \times \left\{ \ln \left[1 - r_{\text{TM}}^2(i\xi_l, k_{\perp})e^{-2aq_l}\right] + \ln \left[1 - r_{\text{TE}}^2(i\xi_l, k_{\perp})e^{-2aq_l}\right] \right\}. \quad (1)$$

Here k_B is the Boltzmann constant and $\xi_l = 2\pi k_B T l / \hbar$ with $l = 0, 1, 2, \dots$ are the Matsubara frequencies ($k_{\perp} = |\mathbf{k}_{\perp}|$ is the projection of a wave vector on the plane of the plates). The reflection coefficients for the two independent polarizations of the electromagnetic field (transverse magnetic and transverse electric) are given by

$$r_{\text{TM}}(i\xi_l, k_{\perp}) = \frac{\varepsilon_l^2 q_l^2 - k_l^2}{\varepsilon_l^2 q_l^2 + k_l^2 + 2q_l k_l \varepsilon_l \coth(k_l d)},$$

$$r_{\text{TE}}(i\xi_l, k_{\perp}) = \frac{k_l^2 - q_l^2}{q_l^2 + k_l^2 + 2q_l k_l \coth(k_l d)}, \quad (2)$$

where

$$q_l = \sqrt{k_{\perp}^2 + \frac{\xi_l^2}{c^2}}, \quad k_l = \sqrt{k_{\perp}^2 + \varepsilon_l \frac{\xi_l^2}{c^2}}, \quad \varepsilon_l = \varepsilon(i\xi_l) \quad (3)$$

and $\varepsilon(\omega)$ is the dielectric permittivity of the plate material.

As was already discussed in the Introduction, in the framework of the Lifshitz theory the calculation results strongly depend on the model of a metal used. The source of discrepancies are different contributions from zero frequency [the term with $l = 0$ in Eq. (1)]. For ideal metal plates it holds $|\varepsilon| = \infty$ at any frequencies, including $\xi_0 = 0$, and from (2) one obtains

$$r_{\text{TM}}(i\xi_l, k_{\perp}) = r_{\text{TE}}(i\xi_l, k_{\perp}) = 1. \quad (4)$$

For metals with $\varepsilon \sim 1/\xi$ when $\xi \rightarrow 0$ (this includes but not reduces to the Drude model) from (2) it follows [13, 23]

$$r_{\text{TM}}(0, k_{\perp}) = 1, \quad r_{\text{TE}}(0, k_{\perp}) = 0. \quad (5)$$

For metals with $\varepsilon \sim \omega_p^2/\xi^2$ when $\xi \rightarrow 0$, where ω_p is the plasma frequency, (2) leads to a qualitatively different result for the transverse electric reflection coefficient [14, 15],

$$r_{\text{TM}}(0, k_{\perp}) = 1, \quad (6)$$

$$r_{\text{TE}}(0, k_{\perp}) = \frac{\omega_p^2}{\omega_p^2 + 2k_{\perp}^2 c^2 + 2k_{\perp} c \sqrt{k_{\perp}^2 c^2 + \omega_p^2} \coth\left(\frac{d}{c} \sqrt{k_{\perp}^2 c^2 + \omega_p^2}\right)}.$$

As is seen from the comparison of (4) and (5), there is a qualitative disagreement in the values of $r_{\text{TE}}(0, k_{\perp})$. This results in hundreds times larger thermal corrections at short separation if one uses (5) instead of (4). At large separations the magnitudes of the Casimir free energy and pressure obtained by using (5) are one half of those when using (4). At the same time all results obtained from (4) and (6) are in qualitative agreement. This is guaranteed by the fact that (6) smoothly approaches (4) when $\omega_p \rightarrow \infty$.

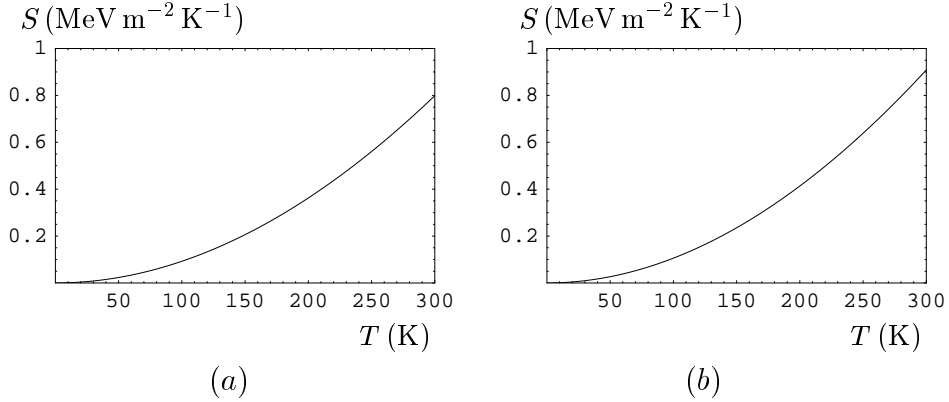


Figure 1. The Casimir entropy for two plates made of an ideal metal (a) and metal described by the plasma model with $\omega_p = 9.0$ eV (b) at a separation 300 nm.

The crucial question for any model used is its consistency with the fundamental physical principles. In our case the considered models of dielectric permittivity can be tested thermodynamically by the behavior of the Casimir entropy,

$$S(a, T) = -\frac{\partial \mathcal{F}(a, T)}{\partial T}, \quad (7)$$

at low temperatures. In figure 1(a) we plot the Casimir entropy as a function of temperature for ideal metals [24, 25] and in figure 1(b) for metals with $\varepsilon \approx \omega_p^2/\xi^2$ when $\xi \rightarrow 0$ [16, 17]. In both cases it holds $S(a, T) \geq 0$ and $S(a, T) \rightarrow 0$ when T vanishes. This means that the Nernst heat theorem is satisfied.

Quite different situation holds for metals with $\varepsilon \sim 1/\xi$ when $\xi \rightarrow 0$. The Casimir entropy for $\varepsilon = 1 + \omega_p^2/[\xi(\xi + \gamma)]$, where γ is the relaxation parameter, is plotted in figure 2(a) [16]. As is seen in this figure, the entropy becomes negative at T of about several hundred K and remains negative

$$S(a, 0) = -\frac{k_B \zeta(3)}{16\pi a^2} \left[1 - 4\frac{c}{\omega_p a} + 12\left(\frac{c}{\omega_p a}\right)^2 - \dots \right] < 0 \quad (8)$$

at $T = 0$ [here $\zeta(z)$ is the Riemann zeta function]. Thus, the Nernst heat theorem is violated, suggesting that the model used is inapplicable. Figure 2(a) is plotted for perfect crystal lattice with no impurities when $\gamma \rightarrow 0$ with $T \rightarrow 0$. In [26, 27] it was argued that the presence of impurities can remedy this situation. However, in [27] the dependence of the relaxation parameter on the temperature was not taken into account. As a result, the coefficients of the obtained asymptotic expressions were determined incorrectly up to factors of several orders of magnitude [28]. For typical realistic concentrations of impurities the behavior of the entropy as a function of temperature remains the same, as in figure 2(a), up to as low temperatures as $10^{-3} - 10^{-4}$ K. At lower temperatures, however, the Casimir entropy depends on T in a different way, as is shown in figure 2(b) for a typical residual resistivity equal to 10^{-4} of the resistivity at room temperature. Although from figure 2(b) it is seen that, at least formally, the Nernst heat theorem is preserved for lattices with impurities, this does not solve the contradiction between the models with $\varepsilon \sim 1/\xi$ and thermodynamics. The point is that, according to quantum

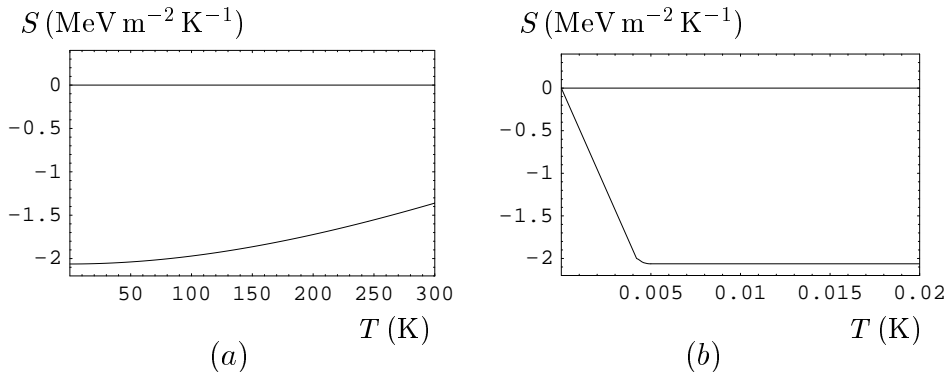


Figure 2. The Casimir entropy for two plates made of Drude metal with perfect crystal lattice (a) and of Drude metal with impurities (b) at a separation $1\mu\text{m}$ ($\gamma = 0.035\text{ eV}$).

statistical physics, the Nernst heat theorem must be valid for perfect crystal lattice which has a nondegenerate dynamic state of lowest energy. Thus, any model that violates this rule is thermodynamically unacceptable.

Another crucial question for any model is consistency with experiment. As is shown in [5, 6, 7], both the plasma model and the impedance approach are consistent with the results of most precise measurements of the Casimir pressure at separations $a \geq 160\text{ nm}$. The same measurement results are, however, inconsistent with the Drude model approach. In figure 3(a) we plot the differences between the theoretical Casimir pressures in the configuration of two parallel plates calculated using the Drude model and tabulated optical data and mean experimental pressures as a function of separation [7]. It is seen that all differences are outside of the 95% confidence intervals whose boundaries generate a solid line. Within a wide separation region from 210 to 620 nm they are also outside of the 99.9% confidence intervals indicated by the dashed line. Thus, the Drude model approach is experimentally excluded. Note that in theoretical computations in figure 3(a) the tabulated optical data were extrapolated to low frequencies by the Drude model with the plasma frequency $\omega_p = 8.9\text{ eV}$ and the relaxation parameter $\gamma = 0.0357\text{ eV}$. Importantly, variations of γ practically do not influence the magnitudes of the Casimir pressure. For example, a decrease of γ until 0.02 eV would lead to only 0.29% increase of $|P_D^{\text{th}}|$ at $a = 200\text{ nm}$ and to 0.26% increase at $a = 650\text{ nm}$. This is because the value of γ does not influence the zero-frequency term of the Lifshitz formula. As a result, the width of separation intervals, where the Drude model approach is excluded, practically does not depend on the value of γ . If the smaller values of ω_p are used (as suggested in [29]), the Drude model approach is excluded at 99.9% confidence level within even wider separation interval.

The plasma model approach, although it agrees with the measurements of [5, 6, 7], also cannot be considered as a universal. In figure 3(b) we plot the differences of the theoretical Casimir forces between a plate and a sphere which are calculated using the plasma model and mean experimental Casimir forces [18] versus separation. It is

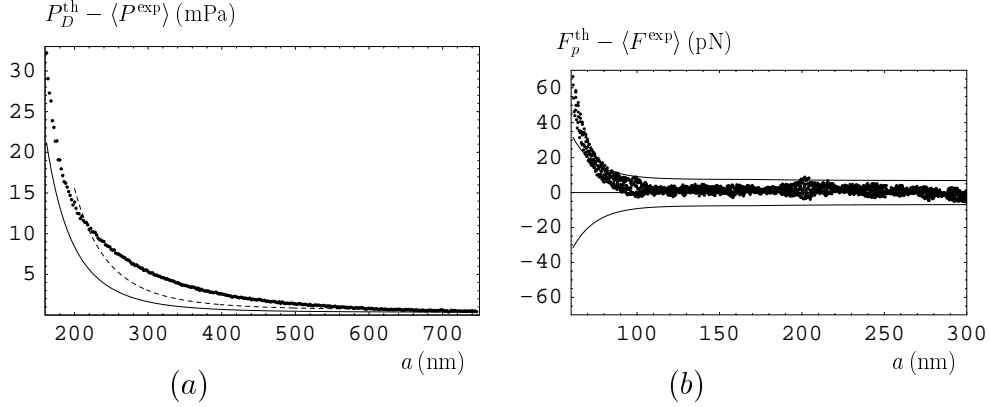


Figure 3. Differences between the theoretical and mean experimental Casimir pressures (a) and forces (b) versus separation. Theoretical quantities are computed using the Drude model and tabulated optical data (a) and plasma model (b). Solid lines and dashed line show the confidence intervals with 95% and 99.9% confidence levels, respectively. In computations the values of the plasma frequency $\omega_p = 8.9$ eV and the relaxation parameter $\gamma = 0.0357$ eV were used, as determined in [7] for Au films deposited on the test bodies from the resistivity measurements.

seen that at separations below 80 nm the plasma model approach is excluded by the experimental data. Bearing in mind that at so short separations (below the plasma wavelength) the impedance approach is not applicable, it may be concluded that until recently there was no theoretical approach to the thermal Casimir force consistent with both long-separation and short-separation experiments. Such an approach based on the generalized plasma-like permittivity was first proposed in [20, 21] and used in [7]. Below we discuss the main points of this approach and apply it to semiconductors of metallic type.

3. Drude model and the effect of finite plates

Before considering the generalized plasma-like permittivity, we briefly discuss the physical reasons why the Drude model dielectric permittivity,

$$\varepsilon_D(\omega) = 1 - \frac{\omega_p^2}{\omega(\omega + i\gamma)}, \quad (9)$$

fails to provide an adequate description of the thermal Casimir force. The idea of this explanation belongs to Parsegian [30] who noticed that the Drude model is derived from the Maxwell equations in an infinite metallic medium (semispace) with no external sources, zero induced charge density and with nonzero induced current $\mathbf{j} = \sigma_0 \mathbf{E}$ (σ_0 is the conductivity at a constant current). In such a medium there are no walls limiting the flow of charges. Physically the condition that the semispace is infinite means that its extension is much longer than the extension of the wave front (recently the role of finite size of the conductors was also discussed in [32] in the case of two wires interacting through the inductive coupling between Johnson currents).

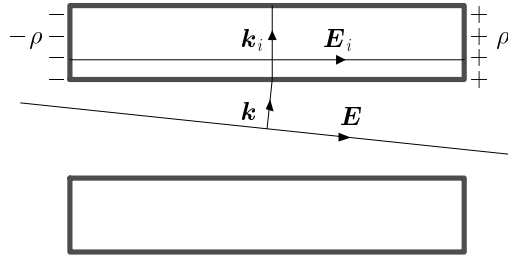


Figure 4. The electromagnetic plane wave of a vanishing frequency with a wave vector \mathbf{k} is incident on a metal plate of finite size leading to the accumulation of charges on its back sides.

For real metal plates, however, the applicability conditions of the Drude model are violated. The extension of the wavefront of a plane wave is much longer than of any conceivable metal plate. For plane waves of very low frequency, the electric field \mathbf{E}_i inside the plate is practically constant and it is parallel to the boundary surface (see figure 4 where \mathbf{k} and \mathbf{k}_i are the wave vectors outside and inside the plate, respectively). Constant electric field \mathbf{E}_i creates a short-lived current of conduction electrons leading to the formation of practically constant charge densities $\pm\rho$ on the opposite sides of the plate (see figure 4). As a result, both the electric field and the current inside the plate vanish. The field outside the plate becomes equal to the superposition of the incident field \mathbf{E} and the field \mathbf{E}_ρ produced by the charge densities $\pm\rho$ [31]. This process takes place in a very short time interval of about 10^{-18} s [21].

One can conclude that a finite metal plate exposed to a plane wave of very low frequency is characterized by zero current of conduction electrons and nonzero induced current density. Thus, it cannot be described by the Drude dielectric function (9). As to the plasma dielectric permittivity obtained from (9) by putting $\gamma = 0$, it leads to zero real current of conduction electrons and admits only a displacement current. Because of this, the plasma model does not allow the accumulation of charges on the sides of a finite plate in the electromagnetic wave of low frequency. Note also that for the plane waves of sufficiently high frequency there is no problem in the application of the Drude dielectric function. Thus, at $T = 300$ K the first Matsubara frequency $\xi_1 = 2.47 \times 10^{14}$ rad/s and for plane waves with $\omega \geq \xi_1$ the electric field \mathbf{E}_i changes its direction so quickly that the average charge densities on the plate sides are equal to zero, in accordance with the applicability conditions of the Drude model.

4. Generalized plasma-like permittivity

The generalized plasma-like dielectric permittivity disregards relaxation of conduction electrons (as does the usual plasma model) but takes into account relaxation processes

of core electrons. It is given by

$$\varepsilon(\omega) = 1 - \frac{\omega_p^2}{\omega^2} + \sum_{j=1}^K \frac{f_j}{\omega_j^2 - \omega^2 - ig_j\omega}, \quad (10)$$

where $\omega_j \neq 0$ are the resonant frequencies of core electrons, g_j are their relaxation parameters, and f_j are the oscillator strengths. The generalized plasma-like permittivity was applied to describe the thermal Casimir force in [20]. As the usual plasma model, permittivity (10) admits only a displacement current and does not allow the accumulation of charges on the sides of a finite plate. It also leads to the same values (6) of the reflection coefficients at zero frequency as the usual plasma model. The values of parameters f_j , ω_j and g_j can be found by fitting the imaginary part of $\varepsilon(\omega)$ in (10) to the tabulated optical data for the complex index of refraction. For example, for Au the results of a 3-oscillator fit ($K = 3$) can be found in [30]. Using the complete data in [22], the more exact 6-oscillator fit ($K = 6$) for Au was performed in [7]. The resulting values of the oscillator parameters are presented in table 1.

Table 1. The oscillator parameters for Au found from the 6-oscillator fit to the tabulated optical data.

j	ω_j (eV)	g_j (eV)	f_j (eV ²)
1	3.05	0.75	7.091
2	4.15	1.85	41.46
3	5.4	1.0	2.700
4	8.5	7.0	154.7
5	13.5	6.0	44.55
6	21.5	9.0	309.6

Equation (10) and table 1 were used together with the Lifshitz formula (1) to calculate the theoretical Casimir pressure in the configuration of two parallel plates and Casimir force in the configuration of a sphere above a plate. The results were compared with the measurement data of [6, 7] and of [18], respectively. The differences of the theoretical and mean experimental Casimir pressures versus separation are shown in figure 5(a) as dots. The differences of the theoretical and mean experimental Casimir forces are shown as a function of separation in figure 5(b). In both figures solid lines represent the borders of the 95% confidence intervals. As is seen in figures 5(a) and 5(b), all dots are well inside the confidence intervals. Thus, the generalized plasma-like dielectric permittivity (10) combined with the Lifshitz formula is consistent with the measurement data of both long- and short-separation measurements of the Casimir force performed up to date.

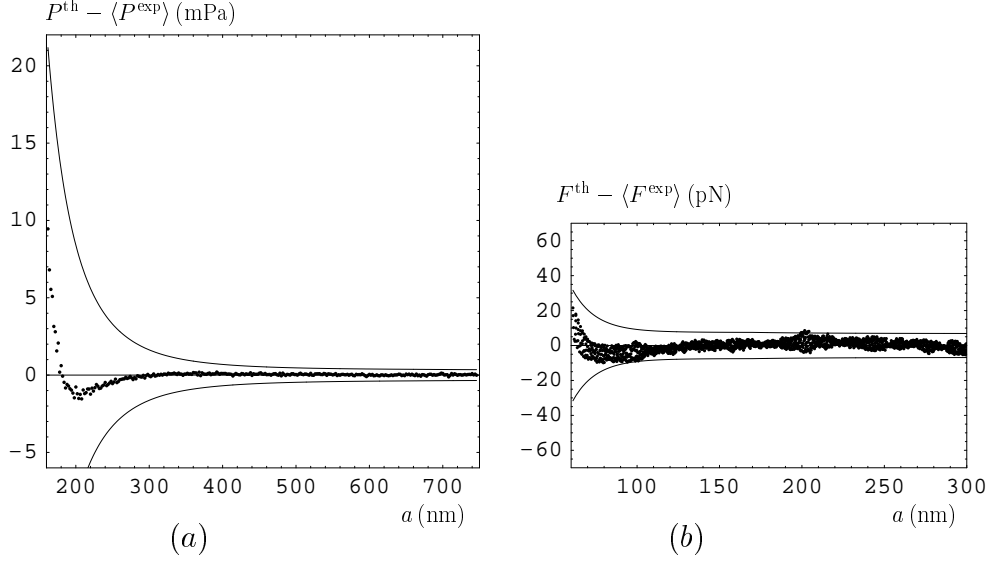


Figure 5. Differences between the theoretical and experimental Casimir pressures (a) and forces (b) versus separation. Theoretical quantities are computed using the generalized plasma-like permittivity (10). Solid lines show the confidence intervals with 95% confidence.

5. Kramers-Kronig relations and their generalizations

An important advantage of the plasma-like dielectric permittivity (10) is that it precisely satisfies the Kramers-Kronig relations. There is some confusion in the literature concerning the Kramers-Kronig relations in the case of usual plasma model which is characterized by entirely real permittivity. In fact the form of Kramers-Kronig relations is different depending on the analytic properties of the considered dielectric permittivity. If $\varepsilon(\omega) = \varepsilon'(\omega) + i\varepsilon''(\omega)$ is regular at $\omega = 0$, the Kramers-Kronig relations take its simplest form [31],

$$\varepsilon'(\omega) = 1 + \frac{1}{\pi} \text{P} \int_{-\infty}^{\infty} \frac{\varepsilon''(\xi)}{\xi - \omega} d\xi, \quad \varepsilon''(\omega) = -\frac{1}{\pi} \text{P} \int_{-\infty}^{\infty} \frac{\varepsilon'(\xi)}{\xi - \omega} d\xi, \quad (11)$$

where the integrals are understood as a principal value.

However, if the dielectric permittivity has a simple pole at $\omega = 0$, $\varepsilon(\omega) \approx 4\pi i\sigma_0/\omega$, the form of the Kramers-Kronig relations is different [33],

$$\varepsilon'(\omega) = 1 + \frac{1}{\pi} \text{P} \int_{-\infty}^{\infty} \frac{\varepsilon''(\xi)}{\xi - \omega} d\xi, \quad \varepsilon''(\omega) = -\frac{1}{\pi} \text{P} \int_{-\infty}^{\infty} \frac{\varepsilon'(\xi)}{\xi - \omega} d\xi + \frac{4\pi\sigma_0}{\omega}. \quad (12)$$

In both cases of being regular and having a simple pole at $\omega = 0$ dielectric permittivity the third dispersion relation, expressing the dielectric permittivity along the imaginary frequency axis, is common:

$$\varepsilon(i\omega) = 1 + \frac{1}{\pi} \text{P} \int_{-\infty}^{\infty} \frac{\xi \varepsilon''(\xi)}{\xi^2 + \omega^2} d\xi. \quad (13)$$

The standard derivation procedure [31, 33], when applied to the dielectric permittivities having a second-order pole at zero frequency [i.e., with an asymptotic

behavior $\varepsilon(\omega) \approx -\omega_p^2/\omega^2$ when $\omega \rightarrow 0$] leads to another form of Kramers-Kronig relations [20],

$$\varepsilon'(\omega) = 1 + \frac{1}{\pi} \text{P} \int_{-\infty}^{\infty} \frac{\varepsilon''(\xi)}{\xi - \omega} d\xi - \frac{\omega_p^2}{\omega^2}, \quad \varepsilon''(\omega) = -\frac{1}{\pi} \text{P} \int_{-\infty}^{\infty} \frac{\varepsilon'(\xi) + \frac{\omega_p^2}{\xi^2}}{\xi - \omega} d\xi. \quad (14)$$

In this case the third Kramers-Kronig relation (13) also is replaced with [20]

$$\varepsilon(i\omega) = 1 + \frac{1}{\pi} \text{P} \int_{-\infty}^{\infty} \frac{\xi \varepsilon''(\xi)}{\xi^2 + \omega^2} d\xi + \frac{\omega_p^2}{\omega^2}, \quad (15)$$

i.e., it acquires an additional term.

It is easily seen that both the usual nondissipative plasma model [given by (9) with $\gamma = 0$] and the generalized plasma-like dielectric permittivity (10) satisfy the Kramers-Kronig relations (14) and (15) precisely.

6. Thermodynamic test for the generalized plasma-like permittivity

As was noted in the Introduction, thermodynamics provides an important test for the used model of dielectric properties. The Casimir entropy computed by using the Lifshitz formula (1) must vanish when the temperature vanishes, i.e., the Nernst heat theorem must be satisfied. This test was used to demonstrate the incompatibility of the Drude model with the Lifshitz formula [16, 17]. The physical reasons for this incompatibility were discussed in Section 3. In [21] the thermodynamic test was applied to the plasma-like dielectric permittivity (10). The low temperature behavior of the Casimir entropy (7) was found analytically under the conditions

$$T \ll T_{\text{eff}} = \frac{\hbar c}{2ak_B}, \quad \alpha \equiv \frac{\lambda_p}{4\pi a} \ll 1, \quad (16)$$

where $\lambda_p = 2\pi c/\omega_p$ is the plasma wavelength. The Casimir entropy is given by

$$\begin{aligned} S(a, T) = & \frac{3\zeta(3)k_B}{8\pi a^2} \left(\frac{T}{T_{\text{eff}}} \right)^2 \left\{ 1 + 4\alpha \right. \\ & - \frac{4\pi^3}{135\zeta(3)} \frac{T}{T_{\text{eff}}} \left(1 + 8\alpha + 6\zeta(3)\alpha^3 \sum_{j=1}^K C_j \delta_j - 96\zeta(3)\alpha^4 \sum_{j=1}^K C_j \delta_j \right) \\ & \left. - \frac{40\zeta(5)}{3\zeta(3)} \left(\frac{T}{T_{\text{eff}}} \right)^2 \alpha^2 \left[1 + 3\alpha \left(\sum_{j=1}^K C_j + 2 \right) - 12\alpha^2 \right] \right\}. \quad (17) \end{aligned}$$

Here, the quantities C_j and δ_j are expressed in terms of the oscillator parameters

$$C_j = \frac{f_j}{\omega_j^2}, \quad \delta_j = \frac{cg_j}{2a\omega_j^2}. \quad (18)$$

Note that in [21] the values of numerical coefficients in the third lines of (38) and (41) are indicated incorrectly. Correct values are obtained by the replacement of all π^2 with $1/12$. In the last term on the right-hand side of (33) in [21] $6/\pi^2$ should be replaced with $1/(2\pi^4)$.

The Casimir entropy defined in (17) is nonnegative. It is seen that

$$S(a, T) \rightarrow 0 \quad \text{when} \quad T \rightarrow 0, \quad (19)$$

i.e., the Nernst heat theorem is satisfied. Thus, the plasma-like dielectric permittivity is not only consistent with all experiments performed up to date, but it also withstands the thermodynamic test.

7. Metal-type semiconductors

The above results are of importance not only for metals but also for metal-type semiconductors. In more detail, the thermal Casimir force between dielectrics and semiconductors is considered in [34]. Here, we briefly discuss only one point, i.e., how to account for the influence of free charge carriers in metal-type semiconductors where the density of these carriers is relatively high.

It is common [22] to include the role of free charge carriers in semiconductors by considering the dielectric permittivity of the form

$$\varepsilon(\omega) = \varepsilon_d(\omega) - \frac{\omega_p^2}{\omega(\omega + i\gamma)}. \quad (20)$$

Here, $\varepsilon_d(\omega)$ is the permittivity of high resistivity (dielectric) semiconductor such that $\varepsilon_d(0) < \infty$. This approach was used for the interpretation of most precise recent experiment on the measurement of the Casimir force between metallic sphere and semiconductor plate by means of an atomic force microscope [9]. In the measurement set under consideration the density of charge carriers in a Si membrane was changed from $5 \times 10^{14} \text{ cm}^{-3}$ to $2.1 \times 10^{19} \text{ cm}^{-3}$ through the absorption of photons from laser pulses. In this differential experiment only the difference of the Casimir forces, ΔF^{exp} , in the presence and in the absence of laser pulse was measured. The experimental data on mean difference forces, $\langle \Delta F^{\text{exp}} \rangle$, was compared with the theoretical difference forces, ΔF^{th} , computed using the Lifshitz theory. In figure 6(a) dots labeled 1 show the quantity $\Delta F^{\text{th}} - \langle \Delta F^{\text{exp}} \rangle$ versus separation, where ΔF^{th} is computed under the assumption that in the absence of laser pulse high resistivity Si is described by $\varepsilon_d(\omega)$, i.e., the effect of dc conductivity is disregarded. Dots labeled 2 show the same quantity, where ΔF^{th} is computed taking into account the dc conductivity of high resistivity Si in the absence of laser pulse. In both cases the dielectric permittivity (20) with appropriate values of ω_p and γ is used when the laser pulse is on. Solid lines indicate the borders of 95% confidence intervals. As is seen in figure 6(a), the Lifshitz theory taking the dc conductivity of high resistivity Si into account is experimentally excluded. The physical explanation for this result can be found in [34]. It is notable also that, as was shown in [35], the inclusion of the dc conductivity of a dielectric in the Lifshitz theory results in the violation of the Nernst heat theorem.

Bearing in mind that the Si plate has finite size, as was discussed in Section 3, a question arises whether the use of the Drude-type dielectric permittivity (20) in the presence of laser pulses for the calculation of the Casimir force is warranted. To

check this point we have recalculated the values of ΔF^{th} versus separation by using the dielectric permittivity $\varepsilon_d(\omega)$ of high resistivity dielectric Si in the absence of laser pulse and the plasma-like permittivity

$$\tilde{\varepsilon}(\omega) = \varepsilon_d(\omega) - \frac{\omega_p^2}{\omega^2} \quad (21)$$

in the presence of pulse. The resulting quantity $\Delta \tilde{F}^{\text{th}} - \langle \Delta F^{\text{exp}} \rangle$ is shown in figure 6(b) as dots labeled 1. As is seen from the comparison of dots labeled 1 in figures 6(a) and 6(b), the use of the generalized plasma-like permittivity (21) leads to a bit better agreement with data than the use of the Drude-type permittivity (20). However, it is not possible to give a statistically meaningful preference to one of the models on these grounds because in both cases most of the dots [of about 95% in figure 6(a) and 100% in figure 6(b)] are inside the confidence intervals.

Thus, although for metals (Au) we already have a decisive confirmation of the fact that the generalized plasma-like permittivity is consistent with experiments on measuring the Casimir force and that the Drude model is excluded, for metal-type semiconductors such confirmation is still lacking. It can be obtained in the proposed, more precise experiments on measuring the difference Casimir force between two sections of a patterned Si plate of different dopant concentration [36].

8. Conclusions and discussion

To conclude, we have demonstrated that the use of the Drude dielectric function in the Lifshitz formula is inconsistent with electrodynamics in the case of finite plates. Instead, to calculate the thermal Casimir force, one should use the generalized plasma-like permittivity that disregards relaxation of free electrons but takes into account

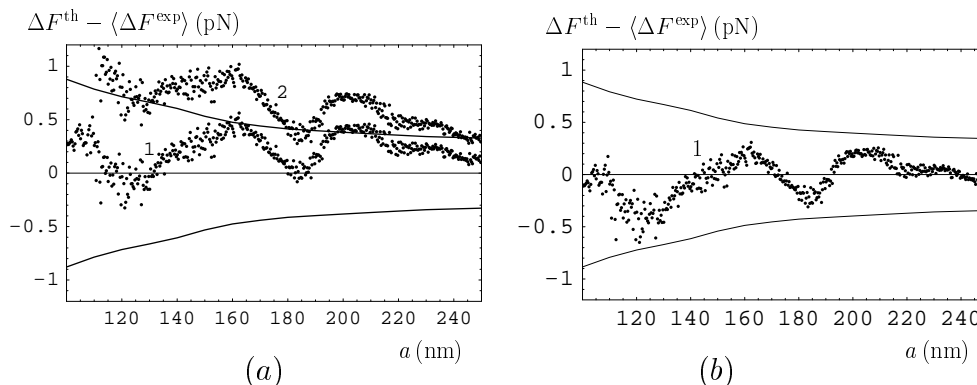


Figure 6. Theoretical minus experimental differences of the Casimir forces versus separation. In the absence of laser pulse the theoretical results for dots labeled 1 are computed using $\varepsilon_d(\omega)$ and for dots labeled 2 taking the dc conductivity of high resistivity Si into account. In both cases $\varepsilon(\omega)$ from (20) is used when the laser pulse is on (a). The same differences labeled 1 calculated using $\varepsilon_d(\omega)$ when the pulse is off and $\tilde{\varepsilon}(\omega)$ from (21) when the pulse is on are shown in (b). Solid lines show the confidence interval with 95% confidence.

relaxation due to interband transitions of core electrons. This permittivity is the only one that is consistent with both short- and long-separation measurements of the Casimir force at $T = 300$ K. The generalized plasma-like permittivity satisfies precisely the Kramers-Kronig relations. The use of this permittivity also leads to a positive Casimir entropy which vanishes at zero temperature in accordance with the Nernst heat theorem. We have also demonstrated that the inclusion of dc conductivity of high resistivity semiconductors is inconsistent with recent experiment on the measurement of the difference Casimir force between metal sphere and Si plate illuminated with laser pulses. We have presented two theoretical descriptions for the dielectric properties of low resistivity Si in the presence of laser pulse by means of the Drude-type and plasma-type permittivities and concluded that available experimental data is not of sufficient precision to discriminate between them. This problem will be solved in the future using results of the proposed experiment [36].

A more fundamental approach to the thermal Casimir force between metals and metal-type semiconductors would require the consideration of finite plates and a more sophisticated description of conduction electrons that is far beyond the scope of the Lifshitz theory.

Acknowledgments

The authors are grateful to G Bimonte, R S Decca, E Fischbach, G L Klimchitskaya, D E Krause, K A Milton and U Mohideen for helpful discussions. VMM is grateful to the Center of Theoretical Studies and Institute for Theoretical Physics, Leipzig University for kind hospitality. This work was supported by Deutsche Forschungsgemeinschaft, Grant No. 436 RUS 113/789/0–3.

References

- [1] Casimir H B G 1948 *Proc. K. Ned. Akad. Wet.* **51** 793
- [2] Bordag M, Mohideen U and Mostepanenko V M 2001 *Phys. Rep.* **353** 1
- [3] Bressi G, Carugno G, Onofrio R and Ruoso G 2002 *Phys. Rev. Lett.* **88** 041804
- [4] Chen F, Mohideen U, Klimchitskaya G L and Mostepanenko V M 2002 *Phys. Rev. Lett.* **88** 101801
Chen F, Mohideen U, Klimchitskaya G L and Mostepanenko V M 2002 *Phys. Rev. A* **66** 032113
- [5] Decca R S, Fischbach E, Klimchitskaya G L, Krause D E, López D and Mostepanenko V M 2003 *Phys. Rev. D* **68** 116003
Decca R S, López D, Fischbach E, Klimchitskaya G L, Krause D E and Mostepanenko V M 2005 *Ann. Phys. NY* **318** 37
Klimchitskaya G L, Decca R S, López D, Fischbach E, Krause D E and Mostepanenko V M 2005 *Int. J. Mod. Phys. A* **28** 2205
- [6] Decca R S, López D, Fischbach E, Klimchitskaya G L, Krause D E and Mostepanenko V M 2007 *Phys. Rev D* **75** 077101
- [7] Decca R S, López D, Fischbach E, Klimchitskaya G L, Krause D E and Mostepanenko V M 2007 *Eur. Phys. J C* **51** 963
- [8] Chen F, Mohideen U, Klimchitskaya G L and Mostepanenko V M 2005 *Phys. Rev. A* **72** 020101(R)
Chen F, Mohideen U, Klimchitskaya G L and Mostepanenko V M 2006 *Phys. Rev. A* **74** 022103

- Chen F, Klimchitskaya G L, Mostepanenko V M and Mohideen U 2006 *Phys. Rev. Lett.* **97** 170402
- [9] Chen F, Klimchitskaya G L, Mostepanenko V M and Mohideen U 2007 *Optics Express* **15** 4823
Chen F, Klimchitskaya G L, Mostepanenko V M and Mohideen U 2007 *Phys. Rev. B* **76** 035338
- [10] Buks E and Roukes M L 2001 *Phys. Rev. B* **63** 033402
- [11] Chan H B, Aksyuk V A, Kleiman R N, Bishop D J and Capasso F 2001 *Science* **291** 1941
Chan H B, Aksyuk V A, Kleiman R N, Bishop D J and Capasso F 2001 *Phys. Rev. Lett.* **87** 211801
- [12] Lifshitz E M 1956 *Sov. Phys. JETP* **2** 73
Dzyaloshinskii I E, Lifshitz E M and Pitaevskii L P 1961 *Sov. Phys. Usp.* **4** 153
- [13] Boström M and Sernelius B E 2000 *Phys. Rev. Lett.* **84** 4757
- [14] Genet G, Lambrecht A and Reynaud S 2000 *Phys. Rev. A* **62** 012110
- [15] Bordag M, Geyer B, Klimchitskaya G L and Mostepanenko V M 2000 *Phys. Rev. Lett.* **85** 503
- [16] Bezerra V B, Klimchitskaya G L, Mostepanenko V M and Romero C 2004 *Phys. Rev. A* **69** 022119
- [17] Bezerra V B, Decca R S, Fischbach E, Geyer B, Klimchitskaya G L, Krause D E, López D, Mostepanenko V M and Romero C 2006 *Phys. Rev. E* **73** 028101
- [18] Harris B W, Chen F and Mohideen U 2000 *Phys. Rev. A* **62** 052109
Chen F, Klimchitskaya G L, Mohideen U and Mostepanenko V M 2004 *Phys. Rev. A* **69** 022117
- [19] Bezerra V B, Klimchitskaya G L and Romero C 2002 *Phys. Rev. A* **65** 012111
Geyer B, Klimchitskaya G L and Mostepanenko V M 2003 *Phys. Rev. A* **67** 062102
Bezerra V B, Bimonte G, Klimchitskaya G L, Mostepanenko V M and Romero C 2007 *Eur. Phys. J. C* **52** 701
- [20] Klimchitskaya G L, Mohideen U and Mostepanenko V M 2007 *J. Phys. A.: Mat. Theor.* **40** F339
- [21] Geyer B, Klimchitskaya G L and Mostepanenko V M 2007 *J. Phys. A.: Mat. Theor.* **40** 13485
- [22] Palik E D (ed) 1985 *Handbook of Optical Constants of Solids* (New York: Academic)
- [23] Høyе J S, Brevik I, Aarseth J B and Milton K A 2003 *Phys. Rev. E* **67** 056116
- [24] Brown L S and Maclay G J 1969 *Phys. Rev.* **184** 1272
- [25] Mitter H and Robaschik D 2000 *Eur. Phys. J. B* **13** 335
- [26] Boström M and Sernelius B E 2000 *Physica A* **339** 53
- [27] Høyе J S, Brevik I, Ellingsen S A and Aarseth J B 2007 *Phys. Rev. E* **75** 051127
- [28] Klimchitskaya G L and Mostepanenko V M 2007 e-print quant-ph/0703214, *Phys. Rev. E* to appear
- [29] Pirozhenko I, Lambrecht A and Svetovoy V B 2006 *New J. Phys.* **8** 238
- [30] Parsegian V A 2005 *Van der Waals forces: A Handbook for Biologists, Chemists, Engineers, and Physicists* (Cambridge: Cambridge University Press)
- [31] Jackson J D 1999 *Classical Electrodynamics* (New York: John Wiley & Sons)
- [32] Bimonte G 2007 *New J. Phys.* **9** 281
- [33] Landau L D, Lifshitz E M and Pitaevskii L P 1984 *Electrodynamics of Continuous Media* (Oxford: Pergamon Press)
- [34] Klimchitskaya G L and Geyer B 2008 *J. Phys. A: Math. Theor.* this issue
- [35] Geyer B, Klimchitskaya G L and Mostepanenko V M 2005 *Phys. Rev. D* **72** 085009
Geyer B, Klimchitskaya G L and Mostepanenko V M 2006 *Int. J. Mod. Phys. A* **21** 5007
Geyer B, Klimchitskaya G L and Mostepanenko V M 2008 *Ann. Phys. NY* **323** 291
- [36] Castillo-Garza R, Chang C-C, Jimenez D, Klimchitskaya G L, Mostepanenko V M and Mohideen U 2007 *Phys. Rev. A* **75** 062114